

1 STANDARD MODEL IS BEST MODEL (WORKING TITLE)

2 William Kennedy DiClemente

3 A DISSERTATION

4 in

5 Physics and Astronomy

6 Presented to the Faculties of The University of Pennsylvania

7 in Partial Fulfillment of the Requirements for the Degree of Doctor of Philosophy

8 2018 Last compiled: December 18, 2018

9

10 I. Joseph Kroll, Professor, Physics
11 Supervisor of Dissertation

12

13 Joshua Klein, Professor, Physics
14 Graduate Group Chairperson

15 Dissertation Committee

16 (Committee Prof. 1), Professor, Physics

17 (Committee Prof. 2), Associate Professor, Physics

18 (Committee Prof. 3), Professor, Physics

19 (Committee Prof. 4), Professor, Physics

20 I. Joseph Kroll, Professor, Physics

21

STANDARD MODEL IS BEST MODEL (WORKING TITLE)

22

COPYRIGHT

23

2018

24

William Kennedy DiClemente

25

All rights reserved.

Acknowledgements

27 I'd like to thanks the Ghosts of Penn Students Past for providing me with such an amazing thesis
28 template.

29

ABSTRACT

30

STANDARD MODEL IS BEST MODEL (WORKING TITLE)

31

William Kennedy DiClemente

32

J. Kroll

33

This is the abstract text.

Contents

35	Acknowledgements	iii
36	Abstract	iv
37	Contents	v
38	List of Tables	viii
39	List of Figures	ix
40	Preface	x
41	1 Introduction	1
42	2 Theoretical Framework	2
43	2.1 Introduction to the Standard Model	2
44	2.2 Electroweak Mixing and the Higgs Field	2
45	3 LHC and the ATLAS Detector	3
46	3.1 The Large Hadron Collider	3
47	3.2 The ATLAS Detector	3
48	3.2.1 The Inner Detector	3
49	3.2.1.1 Pixel Detector	3
50	3.2.1.2 Semiconductor Tracker	3
51	3.2.1.3 Transition Radiation Tracker	3
52	3.2.2 The Calorimeters	4

53	3.2.2.1	Liquid Argon Calorimeters	4
54	3.2.2.2	Tile Calorimeters	4
55	4	Alignment of the ATLAS Inner Detector	5
56	4.1	Effects of Misalignment	5
57	4.2	The Alignment Method	5
58	4.3	Momentum Bias Corrections	5
59	4.4	Alignment of the IBL	6
60	4.5	Alignment Monitoring	6
61	5	WZ production @ $\sqrt{s} = 13$ TeV	7
62	5.1	Theoretical motivation	7
63	5.2	Signal definition	7
64	5.3	Background estimations	7
65	5.4	Cross section measurement	7
66	6	Same-sign WW @ $\sqrt{s} = 13$ TeV	8
67	6.1	Theoretical motivation	8
68	6.2	Signal definition	8
69	6.3	Background estimations	8
70	6.4	Cross section measurement	8
71	7	Prospects for same-sign WW at the High Luminosity LHC	9
72	7.1	Theoretical motivation	9
73	7.2	Signal definition	9
74	7.2.1	Sensitivity to longitudinal polarization	10
75	7.3	Background estimations	10
76	7.4	Selection optimization	10
77	7.4.1	Random grid search algorithm	10
78	7.4.2	Inputs to the optimization	12
79	7.4.3	Results of the optimization	12
80	7.5	Cross section measurement	12
81	8	Conclusion	13

82	Bibliography
----	---------------------

14

List of Tables

List of Figures

85	3.1	General cut-away view of the ATLAS detector.	4
86	7.1	A visual representation of a rectangular grid search algorithm. The signal events are the	
87		blue triangles, and the red circles are the background events. TODO: replace with own	
88		figure	11
89	7.2	A visual representation of a random grid search algorithm. The signal events are the	
90		blue triangles, and the red circles are the background events. TODO: replace with own	
91		figure	11

Preface

93 This is the preface. It's optional, but it's nice to give some context for the reader and stuff.

Will K. DiClemente
Philadelphia, February 2019

95

CHAPTER 1

96

Introduction

97 The Standard Model (SM)¹ has been remarkably successful...

¹Here's a footnote.

98

CHAPTER 2

99

Theoretical Framework

100 (Some example introductory text for this chapter)...

101 **2.1 Introduction to the Standard Model**

102 Modern particle physics is generally interpreted in terms of the Standard Model (SM). This is a
103 quantum field theory which encapsulates our understanding of the electromagnetic, weak, and strong
104 interactions...

105 **2.2 Electroweak Mixing and the Higgs Field**

106 When the theory of the electroweak interaction was first developed [[1](#), [2](#)], the W and Z bosons were
107 predicted to be massless (a typical mass term in the Lagrangian would violate the $SU(2)$ symmetry).
108 However, these were experimentally observed to have masses...

CHAPTER 3

LHC and the ATLAS Detector

3.1 The Large Hadron Collider

The Large Hadron Collider (LHC) [3] is...

3.2 The ATLAS Detector

ATLAS is a general-purpose particle detector...

3.2.1 The Inner Detector

The Inner Detector serves the primary purpose of measuring the trajectories of charged particles...

3.2.1.1 Pixel Detector

The Pixel detector consists of four cylindrical barrel layers and three disk-shaped endcap layers...

3.2.1.2 Semiconductor Tracker

The Semiconductor Tracker uses the same basic technology as the Pixels, but the fundamental unit of silicon is a larger “strip”...

3.2.1.3 Transition Radiation Tracker

The Transition Radiation Tracker is the outermost component of the ID...

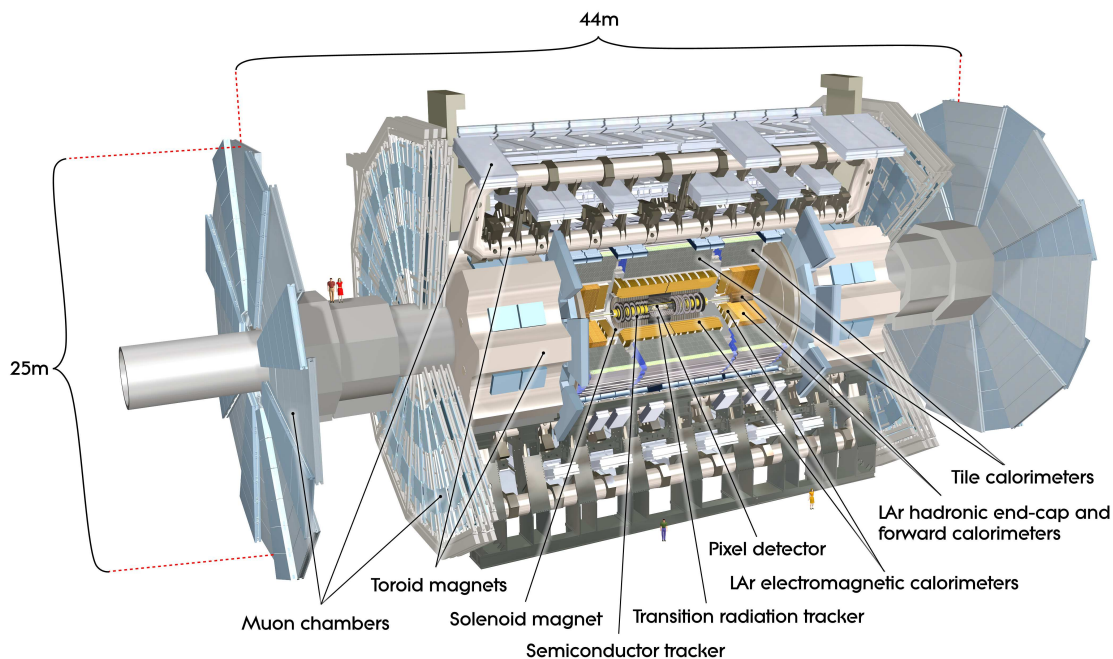


Figure 3.1: General cut-away view of the ATLAS detector [4].

3.2.2 The Calorimeters

ATLAS includes two types of calorimeter system for measuring electromagnetic and hadronic showers. These are the Liquid Argon (LAr) calorimeters and the Tile calorimeters. Together, these cover the region with $|\eta| < 4.9$...

3.2.2.1 Liquid Argon Calorimeters

The Liquid Argon system consists of...

3.2.2.2 Tile Calorimeters

The Tile calorimeter provides coverage for hadronic showers...

CHAPTER 4

Alignment of the ATLAS Inner Detector

In order for the subdetectors of the ID to operate at their designed precisions, it is essential that the locations of the sensors be known as precisely as possible. Differences between the expected and actual positions of a sensor can result in displaced particle hits and degrade track reconstruction quality. These misalignments can occur for any number of reasons, including but not limited to elements shifting during maintenance periods or cycles in ATLAS's magnetic field, or simply small movements during normal detector operations. Since it is not practical to physically realign hundreds of thousands of detector elements to μm precision by hand, an iterative track-based alignment algorithm is used to determine the physical positions and orientations of these elements [5]. The effects of misalignments and the steps taken to correct and monitor them are detailed in this chapter.

4.1 Effects of Misalignment

Hello world!

4.2 The Alignment Method

Hello world!

4.3 Momentum Bias Corrections

Hello world!

149 **4.4 Alignment of the IBL**

150 Hello world!

151 **4.5 Alignment Monitoring**

152 Hello world!

153

CHAPTER 5

154

WZ production @ $\sqrt{s} = 13$ TeV

155 **5.1 Theoretical motivation**

156 Hello world!

157 **5.2 Signal definition**

158 Hello world!

159 **5.3 Background estimations**

160 Hello world!

161 **5.4 Cross section measurement**

162 Hello world!

163

CHAPTER 6

164

Same-sign WW @ $\sqrt{s} = 13$ TeV

165 6.1 Theoretical motivation

166 Hello world!

167 6.2 Signal definition

168 Hello world!

169 6.3 Background estimations

170 Hello world!

171 6.4 Cross section measurement

172 Hello world!

CHAPTER 7

Prospects for same-sign WW at the High Luminosity LHC

On December 3, 2018, Run 2 of the LHC officially ended, and the collider was shut down to begin the first of two scheduled extended maintenance periods [6]. During these two long shutdowns, the Phase-I and Phase-II upgrades of the LHC and ATLAS will occur in order to prepare for the High-Luminosity LHC (HL-LHC) which is scheduled to begin operation in 2026 [7].

The HL-LHC is planned to run at an instantaneous luminosity of $\mathcal{L} = 5 \times 10^{34} \text{ cm}^{-2}\text{s}^{-1}$ with an average of 140 collisions per beam-crossing. Over the course of operation, the HL-LHC is expected to collect a total integrated luminosity of $\mathcal{L} = 3000 \text{ fb}^{-1}$ by 2035 [8].

These run conditions are much harsher than what ATLAS has experienced so far, and as a result there are several planned upgrades to the detector. Most notably, the entire ID will be replaced with an all-silicon tracker which will extend the coverage from $|\eta| \leq 2.7$ up to $|\eta| \leq 4.0$. This will allow for reconstruction of charged particle tracks which can in turn be matched to clusters in the calorimeters for electron identification or forward jet tagging [9].

TODO: Why are we studying ssww at the HL-LHC

7.1 Theoretical motivation

The theoretical motivation for studying the ssWW process is detailed in Section 6.1.

7.2 Signal definition

Hello world!

7.2.1 Sensitivity to longitudinal polarization

7.3 Background estimations

Hello world!

7.4 Selection optimization

TODO: Motivation

7.4.1 Random grid search algorithm

The chosen algorithm for optimizing the event selection is known as the Random Grid Search (RGS) [10]. Consider a simple case of two variables x and y chosen to differentiate the signal from the background. In order to be considered a signal event, a given event would be required to pass a *cut point* $c = \{x > x_c, y > y_c\}$. A simple method to choose the optimal cut point (i.e. the “best” values of the cuts x_c and y_c) would be to construct an $n \times m$ rectangular grid in x and y consisting of points $(x_0, y_0), (x_1, y_1), \dots, (x_n, y_m)$, as in Figure 7.1. One can then choose a cut point $c_k = \{x > x_i, y > y_j\}$ that maximizes the signal significance as measured by a chosen metric. This would be considered a *regular* or *rectangular* grid search.

While effective in principle, this rectangular grid search comes with two major drawbacks:

1. The algorithm does not scale well as the number of variables to be optimized—the dimensionality of the grid—increases. In the case of a square grid with N bins per variable v , the number of cut points to be evaluated grows as N^v .
2. Signal and background samples are rarely evenly distributed over the entire grid, resulting in many cut points being sub-optimal and evaluating them would be a waste of computing resources.

To combat these limitations, the RGS algorithm constructs a grid of cut points directly from the signal sample itself. In the two-dimensional example, this means that the variables x_i and y_j making up the cut point $c_k = \{x > x_i, y > y_j\}$ take their values directly from a given signal event. This has the benefit of creating a *random grid* of cut points that is by construction biased towards regions of high signal concentration. This reduces the need for exponentially increasing numbers of cut points while ensuring that computing resources are not wasted in regions with few to no signal events. An example of the the two-dimensional random grid is shown in Figure 7.2.

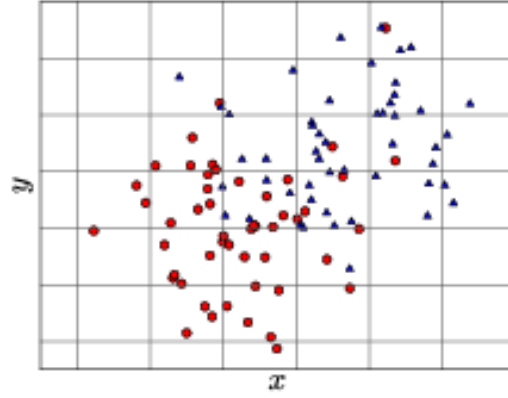


Figure 7.1: A visual representation of a rectangular grid search algorithm. The signal events are the blue triangles, and the red circles are the background events. **TODO: replace with own figure**

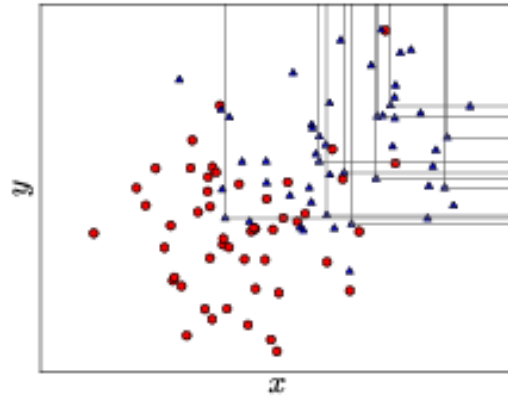


Figure 7.2: A visual representation of a random grid search algorithm. The signal events are the blue triangles, and the red circles are the background events. **TODO: replace with own figure**

7.4.2 Inputs to the optimization

Since the measurement of longitudinally polarized $W^\pm W^\pm jj$ production is the focus of the upgrade study, the random grid was constructed using the LL-polarized events rather than the inclusive EWK production. The variables chosen for optimization are:

- Leading lepton p_T
- Dilepton invariant mass (m_{ll})
- Leading jet p_T
- Subleading jet p_T
- Dijet invariant mass (m_{jj})
- Lepton-jet centrality (ζ)

7.4.3 Results of the optimization

7.5 Cross section measurement

Hello world!

234

CHAPTER 8

235

Conclusion

236 Here’s where you wrap it up.

237 **Looking Ahead**

238

239 Here’s an example of how to have an “informal subsection”.

Bibliography

- [1] S. L. Glashow, *The Renormalizability of Vector Meson Interactions*, *Nucl. Phys.* **10** (1959) 107–117. 2.2
- [2] A. Salam and J. C. Ward, *Weak and Electromagnetic Interactions*, *Nuovo Cimento* **11** (1959) 568–577. 2.2
- [3] L. R. Evans and P. Bryant, *LHC Machine*, JINST **3** (2008) S08001.
<https://cds.cern.ch/record/1129806>. This report is an abridged version of the LHC Design Report (CERN-2004-003). 3.1
- [4] ATLAS Collaboration, *The ATLAS Experiment at the CERN Large Hadron Collider*, JINST **3** (2008) S08003. 3.1
- [5] ATLAS Collaboration Collaboration, *Alignment of the ATLAS Inner Detector Tracking System with 2010 LHC proton-proton collisions at $\sqrt{s} = 7$ TeV*, Tech. Rep. ATLAS-CONF-2011-012, CERN, Geneva, Mar, 2011.
<https://cds.cern.ch/record/1334582>. 4
- [6] R. Steerenberg, *LHC Report: Another run is over and LS2 has just begun...*,
<https://home.cern/news/news/accelerators/lhc-report-another-run-over-and-ls2-has-just-begun>, 2018. Accessed: 2018-12-14. 7
- [7] *Letter of Intent for the Phase-I Upgrade of the ATLAS Experiment*, Tech. Rep. CERN-LHCC-2011-012. LHCC-I-020, CERN, Geneva, Nov, 2011.
<http://cds.cern.ch/record/1402470>. 7
- [8] G. Apollinari, I. Bjar Alonso, O. Brning, M. Lamont, and L. Rossi, *High-Luminosity Large Hadron Collider (HL-LHC): Preliminary Design Report*. CERN Yellow Reports: Monographs. CERN, Geneva, 2015. <https://cds.cern.ch/record/2116337>. 7
- [9] ATLAS Collaboration Collaboration, ATLAS Collaboration, *ATLAS Phase-II Upgrade Scoping Document*, Cern-lhcc-2015-020, Geneva, Sep, 2015.
<http://cds.cern.ch/record/2055248>. 7
- [10] P. C. Bhat, H. B. Prosper, S. Sekmen, and C. Stewart, *Optimizing Event Selection with the Random Grid Search*, *Comput. Phys. Commun.* **228** (2018) 245–257, [arXiv:1706.09907](https://arxiv.org/abs/1706.09907) [hep-ph]. 7.4.1